Investigation on the diffraction of a medium scale gaseous deflagration pressure wave behind a protective wall

Laure Heudier [a], Guillaume Lecocq [a], Yann Grégoire [a], Christophe Proust [a,b]
[a]: INERIS, Verneuil-en-Halatte, France
[b]: UTC, Compiègne, France

1 Introduction

SEVESO industrial sites are suspected to produce major accidents, as for instance explosions, meaning that the disruptive effects of the blast wave may significantly impact the neighborhood. Despite effective mitigation measures may be taken, some residual risks exist which sometimes requires a protection of the buildings. In the specific case of blast, walls may be constructed to try and shelter important buildings. This kind of technique was developed decades ago in the pyrotechnical/ammunition industry for instance to avoid the transmission of an accidental explosion from a depot to the next one [1]. The protection is often a bund which characteristic sizes (thickness, height…) are much larger than that of the pressure wave. In the case of SEVESO industrial sites, the blast originates from a vapor cloud explosion, not from a detonation, so that not only the form of the pressure wave is different ("N" type rather than "triangular") but also its duration, usually longer by orders of magnitude [2]. The duration of the wave might be hundreds of ms so that the wavelength of the wave amounts easily tens of m, larger than the characteristic dimensions of a bund. What kind of protection a blast wall would be able to offer in such circumstances? This specific aspect was investigated experimentally and a tentative interpretation is proposed using a CFD tool.

2 Experiments

Medium-scale experiments with gaseous deflagration and a blast wall were performed. The experimental setup is a 1.5 m diameter polyethylene hemispherical balloon (thickness 150 µm) erected on a 3.5 m² and 1.5 mm thick metal plate. During the preparation of the mixture, this tent is applied against a frame of aluminium rods using a rubber cable maintained in tension by an electromagnet. The magnet (thus the rubber cable) is released just before ignition so that the tent is not maintained anymore and can be pushed freely by the expanding flame. Gas injection and mixing is obtained using Venturi blowers, placed on the platform. This way homogenous and well controlled mixtures could be obtained (which was verified). The

Correspondence to: laure.heudier@ineris.fr

gas concentration is controlled at 2 different locations with 2 oxygen analyzers (Servomex). The mixture is ignited on the vertical axis of the balloon, 5 cm above the platform with a pyrotechnical match (energy of 60 J). In the present paper, the case of 40% H2, 20% 02, 40% N2 mixture is presented with a burning velocity of 3.5 m/s, and a calculated expansion rate of 7.8. A 2 m high and 6 m long wall (10 cm thick) is placed 10 m from the centre of the experimental platform (Fig.1) to mimic the behaviour of a blast wall.

Figure 1: test platform with hemispherical balloon and protective wall of 6m length, 10 m between both

Pressure sensors are placed inside the tent (middle of the platform), at 10 m from the platform (at the same distance than the wall but in another direction), on the front face of the wall, on its rear face and in its shade (at a height of 1 m, at 1 m, 2,5 m, 5 m and 10 m behind the wall). Free-field tests were also performed with the sensors located between 10 and 20 m from the ignition location.

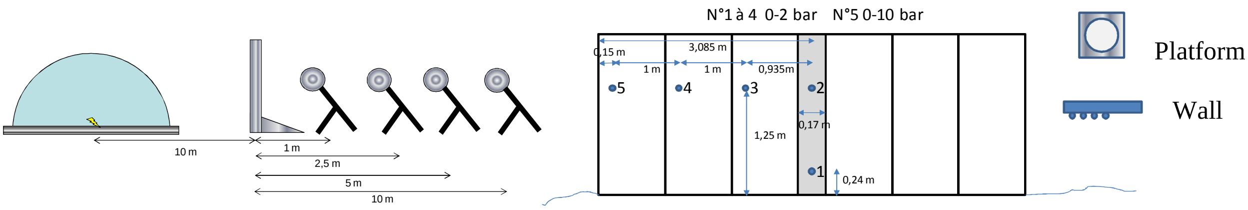

Figure 2: Location of pressure sensors in the shade and on the rear face of protective wall (the wall was reversed for incident directly impacting pressure wave measurements)

3 Numerical Modeling

Numerical modeling was performed using the open source CFD tool OPENFOAM in view of obtaining a deeper understanding of the physics at stake. In OPENFOAM, a modified version of the rhoCentralFoam is used in which the inviscid transport equations of density, momentum, energy and chemical species are solved. An Euler scheme and the Tadmor and Kurganov scheme [3] are used for time integration and discretization of the convection operators. The physical closure of the chemical source terms is written to ensure the volume of burnt gases increases spherically, the time evolution of the radius being set by the modeler. This imposed flame front velocity transforms the fresh gases in burnt products at a user-specified rate and generates a pressure wave. The flame velocity profile is extracted from the experiments. The computational domain is 80 m long, 45 m wide and 40 m high, filled with hexahedra with a characteristic length of a few cm in the zone of interest. Note this approach is intrinsically limited to spherical flame propagation for which the time history of the flame velocity can be known.

4 Results-without the wall

A specific image processing algorithm based on background removal [4], was used to track the flame trajectory (white dashed line in Fig.3) from which the flame velocity was extracted and confronted to the internal pressure trace (Fig. 4).

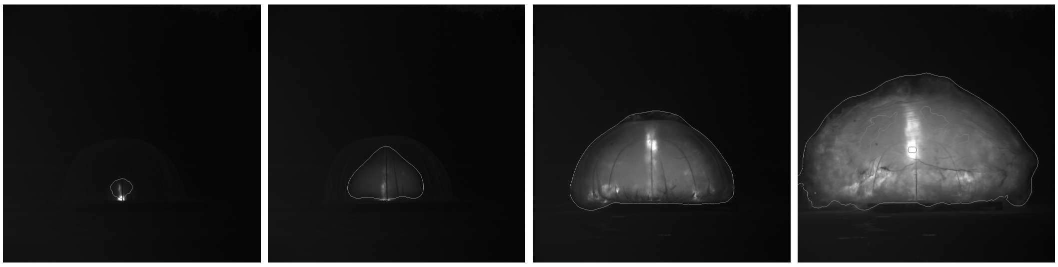

Figure 3: Processed images of the deflagration of the flammable mixture (10 ms between frames).

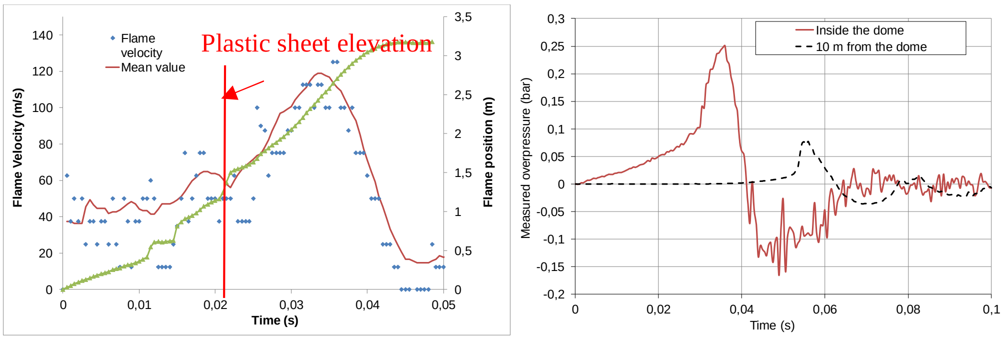

Figure 4: Left: flame trajectory (green dots) and velocity (blue dots and red line) on the vertical axis extracted from the film. Right: Overpressure measured by sensors inside the dome and 10m from the dome

The time evolution of the velocity presents two distinct parts. In the first part, up to about 20-25 ms, the flame velocity is reasonably constant (45 m/s), which is consistent with the linear rise of the overpressure in the burnt gas until 22 ms. The velocity then increases from 45 to 115 m/s. The beginning of this strong acceleration seems to be linked to the motion of the plastic sheet. Its elevation creates a flame acceleration most likely due to a creation of a turbulent/shear flow zone between the flame front and the plastic enveloppe. This leads to a slope change in the pressure signal with significant evolution up to 250 mbar at 36 ms [4]. At 10 m from the dome the free-field pressure peak is 75 mbar, which is consistent with the predicted decrease of overpressure versus distance calculated with multi-energy method [5].

CFD modeling of this reference free-field pressure wave propagation was performed using the experimental flame trajectory as a generator for the pressure wave. CFD simulations show that the input flame trajectory has a direct influence on the shape of the pressure signal in free field. The overpressure peaks were recovered but the positive phase durations were slightly underestimated (10 % on the decaying part). The x-t diagrams of experimental and calculated wave propagation superpose relatively well. This agreement becomes poorer at larger distances because of the model diffusivity. A double overpressure peak, can be noticed at all positions. This is due to the implemented model: the experimental signal of the flame front position was approximated with a set of polynomials in OPENFOAM. The small discontinuity observed at the time of plastic sheet separation is propagated in free field as a dual peak signal. Note that the mesh convergence has been checked systematically for those simulations.

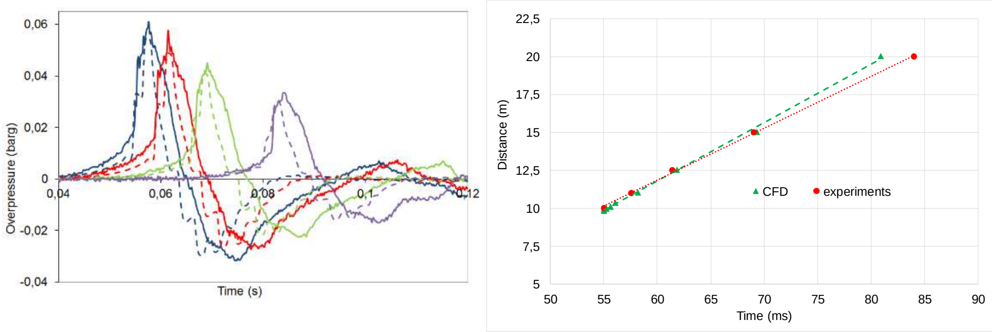

Figure 5: Left : Measured (lines) and CFD predicted (dots) overpressure between 11 and 20 m. Right: x-t diagrams of wave propagation

5 Results- with the wall

In the present experimental configuration, the wavelength of the blast wave (3 m, positive phase duration of 8 ms, see Fig.5L) is comparable to the characteristic dimensions of the wall. Two distinct pressure peaks (Figure 6L) are measured by the 5 sensors on the front face of the wall. This double peak is roughly synchronized on all of the sensors, located either à 24 cm either at 1.25 m from the ground so it cannot be due to a ground reflection. It is more likely due to a rarefaction wave propagating from the top in the compressed zone before the wall (about 3m long). Two peaks are also predicted by the CFD modeling but they are due to the initial flame development in the fireball. The overpressure measured on the front face of the wall are 2 to 3 times higher than the free-field reference measurements (75 mbar at 10 m). Calculated reflection coefficient are slightly below (between 1.5 and 2 with CFD calculations and around 2 with shock wave theory as shown on Fig.6R) [6].

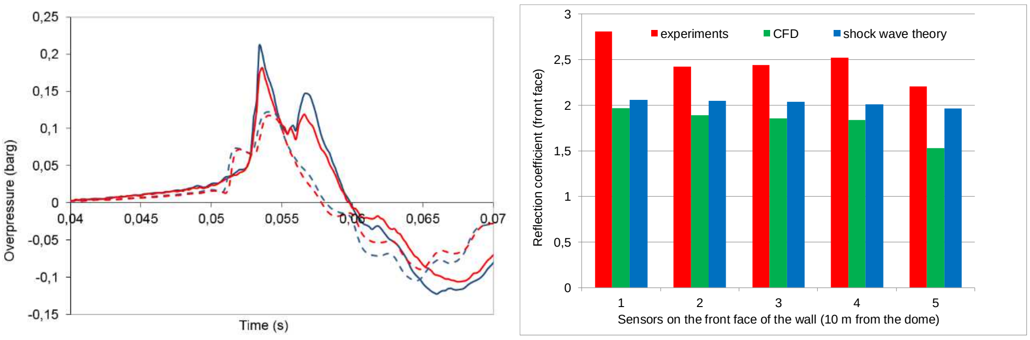

Figure 6: Left: Experimental (line) and calculated (dash line) pressure signals on sensors 1 (blue) and 2 (red) on the front face of wall. Right: Reflection coefficients on each wall sensor

Measurements at the rear face are compared with CFD estimations in Fig.7L. For both sensors, the shape of the experimental signal is recovered in the CFD modeling. Nevertheless, the peaks underestimation is about 30 %. Peaks measured at 0,075s and 0,085s are artefacts, interferences in the measurements and should be ignored. Again the shock attenuation coefficients measured experimentally, computed with the CFD tool and estimated with the theoretical model, are compared in Fig7R.

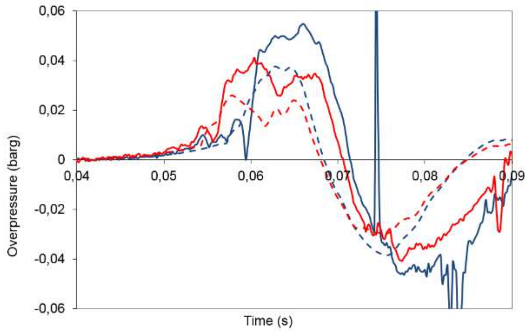

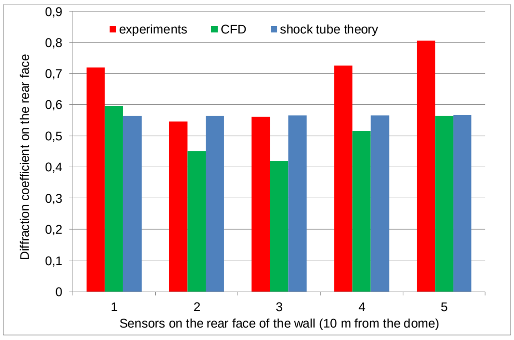

Figure 7: Left: experimental (line) and numerical (dash line) pressure signals on sensor 1 (blue) and 2 (red) on the rear face of wall. Right: overpressure measured and diffraction coefficients on the rear face of wall

Calculated coefficients (between 0,4 and 0,6 with CFD and between 0,5 and 0,6 with shock tube theory) are slightly below observed coefficients (around 0,5-0,8). As expected, the overpressure on the rear face is lower compared to the free-field case, because of the diffraction phenomenon.

The pressure signals measured in the shade of the protection wall, are compared with the CFD predictions in Fig8a. Again the interaction between the incident pressure waves is recovered by the CFD modeling: two peaks are observed and modeled 1 m and 2.5 m behind the wall, but 5 m and 10 m from the wall, a single pressure peak is obtained. The numerical underestimation for all pressure peaks is about 30 %. As before, the blast attenuation coefficients are compared between each measurement type in Fig.8b.

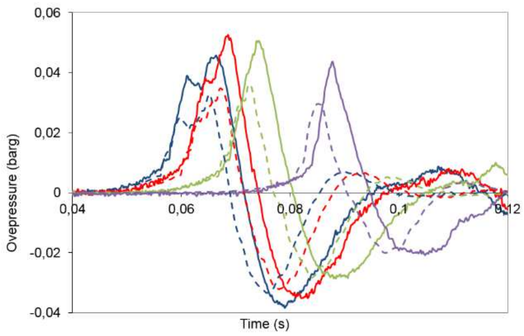

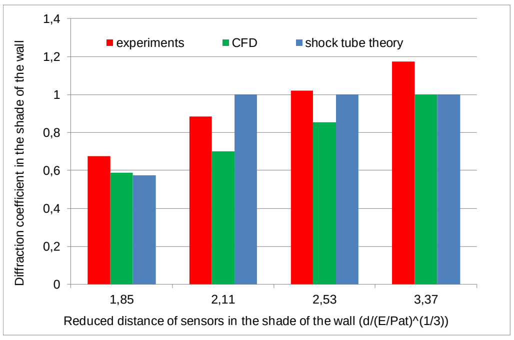

Figure 8: Left: experimental (line) and numerical (dash line) pressure signals l m (blue), 2.5 m (red), 5 m (green) and 10 m (purple) behind the wall. Right: overpressure measured and reduction coefficients behind the wall

Until 2,5 m behind the wall, the overpressure is slightly lower than in free-field case at the same distance. At larger distances from the explosion source the wall has no more influence (diffraction coefficient ~1). Both experiments and calculations indicate that protected length behind the wall is relatively limited (around 3 m). Fig.9L is a schematic representation of a planar pressure wave diffraction around an obstacle. This phenomenon occurs through lateral and top overturning of the wall. Consequently, the compression wave behind the wall may arrive from the top or lateral overturning of the wall which involves that a wall can be protective, for a given height, only if its length is sufficient. In the opposite case the lateral overturning would balance the diffraction on the top of the wall, and reduce the protective effect. Overpressure measured 10 m behind the wall is 1,2 time higher than in free-field. This might be explained by the competition between reduction of overpressure with the increase of distance due to overturning of the obstacle and overlapping of blast waves behind the obstacle. In such situation the CFD results analysis can shed light on the observed events (Fig.9R).

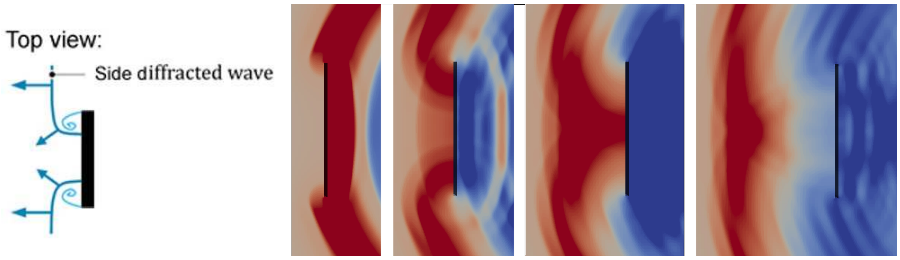

Figure 9: Left: Schematic representation of diffracted wave around an obstacle [7]. Right: Overpressure calculated with OPENFOAM between 50 and 65 ms (overpressure scale from -30 mbar (blue) to 30 mbar (red))

Due to the dimensions of the wall, the lateral overturning wave reaches the rear of the wall, between 5 and 1 ms (depending on sensors location) after the arrival of the top-overturning wave. The positive phase duration of the free-field overpressure wave is close to 10 ms, which is higher than the time difference between lateral and top overturning. Thus, it is very likely that the two waves (side and top overturning) have been summed during experiments. This effect is most likely at the origin of the double peak (top and side overturning) and the positive time duration observed on the two first sensors behind the wall (1 and 2.5 m behind the wall). It can also explain the relatively high peak measured on the first sensor (additional ground reflection effect). Despite blast wave decay with propagation distance, the overlapping effect might lead to overpressure behind a wall, larger than in a free-field case, which could be at the origin of the measurement in Fig.8R. The underestimated impulse in the CFD calculations might explain why this effect is limited in the numerical investigation. Deeper analysis with the CFD tool will be performed in view of quantifying this phenomenon of wave overlapping behind the wall.

In conclusion, this study suggests that the protection provided by a blast wall is very dependent on the wall size compared to the wave size. It shows also that it is theoretically possible to find areas behind the wall where overpressure could be higher than in free-field (that is without any wall), because of the waves recombination. A numerical parametric study and another specific experimental campaign would improve understanding of that point.

References

[1] OTAN, (2006). Manuel sur les principes de sécurité OTAN applicables au stockage des munitions et des explosifs militaires, AASTP-1, 1ère édition

[2] Grégoire Y., (2014). Characterization of pressure signals generated by industrial explosions: incident blast wave. European research project BASIS (Blast Actions on Structures In Steel)

[3] Kurganov A. et al., New High-Resolution Central Schemes for Nonlinear Conservation Laws and Convection–Diffusion Equations, Journal of Computational Physics 160: 241

[4] Daubech J., Proust Ch. Lecocq G., (2015). Turbulent flame propagation in large unconfined H2/O2/N2 clouds, ICHS

[5] Van den Berg, (1984). The Multi-Energy Method – a framework for vapor cloud explosion blast prediction, TNO Prints Maurits Laboratory, report PML 1984-C7

[6] Wright J. K., (1961). Shock Tubes, Methuen & Co LTD, London; John Wiley & sons INC, New York

[7] Baker W.E., Cox P.A., Westine P.S., Kulesz J.J., and Strehlow R.A. (1983). Explosion hazards and evaluation. Fundamental Studies in Engineering. Elsevier, New-York